Proceedings of the 2007 IEEE Symposium on Computational Intelligence in Image and Signal Processing (CIISP 2007)

Robust Object Extraction and Change Detection in Retinal Images for Diabetic Clinical Studies

Qin Li, Jane You, *Member, IEEE*, Lei Zhang, *Member, IEEE*, and Prabir Bhattacharya, *Fellow, IEEE*

***Abstract*—With the rapid advances in computing and electronic imaging technology, there has been increasing interest in developing computer aided medical diagnosis systems to improve the medical service for the public. Images of ocular fundus provide crucial observable features for diagnosing many kinds of pathologies such as diabetes, hypertension, and arteriosclerosis. A computer-aided retinal image analysis system can help eye specialists to screen larger populations and produce better evaluation of treatment and more effective clinical study. This paper is focused on the immediate needs for clinical studies on diabetic patients. Our system includes multiple feature extraction, robust retinal vessel segmentation, hierarchical change detection and classification. The output throughout this system will assist doctors to speed up screening large populations for abnormal cases, and facilitate evaluation of treatment for clinical study.**

I. Introduction

With the fast advances in computing technology and computer industry, multimedia data such as digital signal, image, document, audio, graphics, and video have become widely used in different areas. The aim of the development of automatic medical diagnosis systems for medical applications is to provide storage, processing, and communication services required by the medical community effectively and reliably. Reliable and accurate medical diagnosis requires knowledge of changes in different clinical symptoms due to health degeneration and disease deterioration. One of the main critical issues of such systems is the handling of multimedia medical information in a uniform way to analyze medical data accurately and diagnose different diseases reliably. Image processing techniques offer the means to acquire digital information, at different scales, quickly and efficiently.

This paper is focused on the immediate needs for clinical studies on diabetic patients. To tackle key issues in image understanding, we propose to investigate, design, analyze, implement and evaluate new algorithms for feature extraction, segmentation, region representation and classification. The proposed system includes extracting multiple image features via wavelet transforms; segmenting images based on fuzzy compactness measures; and hierarchical change detection using fuzzy post classification techniques. The feasibility of the proposed system is demonstrated by mapping and analyzing changes caused by disease deterioration in regions of optical eye texture images.

Images of the ocular fundus tell us about retinal, ophthalmic, and even systemic diseases such as diabetes, hypertension, and arteriosclerosis. Previous object extraction works have been done in [7] [18] [19] [20]. The useful objects to monitoring diabetic patients in retinal images include 1) blood vessels, 2) blobs brighter than blood vessels, 3) blobs darker than blood vessels, 4) the optic nerve, and 5) the fovea. An important feature in such diagnoses is the appearance of blood vessels in ocular fundus. Especially the vessels around optic nerve have critical information about diabetic patients. However, automated retinal segmentation is complicated by the fact that the width of retinal vessels can vary from very large to very small, and that the local contrast of vessels is unstable, especially in unhealthy ocular fundus. Previous vessel segmentation methods were either window-based [1] [2] [3] or tracking based [4] [5] [6]. Window-based methods explore the properties of a pixel's surrounding window and emphasize those pixels whose surrounding window matches a given model. Most window-based methods implement classical line detection techniques on vessel fields. In [1], the cross section of a vessel is modeled by a Gaussian shaped curve and the matched filters of 12 directions are used to emphasize vessels. Tracking-based methods utilize a vessel profile model, starting from a number of initial points and incrementally tracing a path that best matches the profile model. In [4], the tracking starts from the papilla, and then is followed with the consideration of the continuities of position, curvature, diameter, and density. In [6], the tracking is improved using a fuzzy model of a vessel profile. In [7], the window-based and tracking-based techniques are integrated and are improved using local region-based threshold probing. In our system we propose a novel vessel segmentation method that includes a multiscale analysis scheme using Gabor filters and scale production. Our method is not only good for detecting large and small vessels concurrently, it is also efficient for denoising and for enhancing the responses of line filters, allowing the detection of vessels with low local contrast.

After object extraction, change detection is performed. This procedure provides information for treatment evaluation and clinical studies. The traditional approaches to

Manuscript received October 13, 2006

Qin Li, Jane You, and Lei Zhang are with the Department of Computing, The Hong Kong Polytechnic University, Hong Kong (852-2766-7309; fax: 852-2766-7309; e-mail: csqinli@ comp.polyu.edu.hk).

Prabir Bhattacharya is with the Institute for Information Systems Engineering, Concordia University, Quebec, Canada (email: prabir@ciise.concordia.ca).

change detection include statistical methods [21], image differencing [22], and post classification comparison approach [23]. Unfortunately, these methods have generally shown relatively poor accuracy because of the classification errors compound in the change detection process [24].

We introduce a wavelet-based hierarchical scheme which integrates fuzzy set theory and image understanding techniques for knowledge discovery of the remote image data. The proposed approach includes algorithms for hierarchical change detection, region representations and classification. The effectiveness of the proposed algorithms is demonstrated throughout the completion of three tasks, namely hierarchical detection of change by fuzzy post classification comparison, localization of change by B-spline based region representation, and categorization of change by hierarchical texture classification.

II. Object Extraction

A. Vessel Detection

Traditional line detection methods proceed either by finding parallel edges [8] [9] or by finding ridges [10] [11] [12]. Parallel edge detection makes use of a bar-shaped model of lines. In [8], a pair of edge detectors was used to detect the left and right edges of a line:

$$E_l(x) = -G'_\sigma\left(x + \frac{w}{2}\right) \quad (1)$$

$$E_r(x) = G'_\sigma\left(x - \frac{w}{2}\right) \quad (2),$$

where w is the width of the line, $G'_\sigma(x)$ is the first derivative of Gaussian and σ is the standard derivation. The responses of E_l and E_r are then nonlinearly combined to give the line response.

Ridge-based detection methods usually use Gaussian-shaped line model. In [10], the ridges are defined as the points on the image where the curvature is the maximum. The second derivate of Gaussian $G''_\sigma(x)$ is often used as a line detector.

One very important factor in line detection is the scale of the filter. To generate a single maximum response on the center of a line, the widths of the filter and the line should be constrained in a proper ratio. For example, the methods described above have to hold

$$\sigma \geq \frac{w}{\sqrt{3}} \quad (3)$$

for bar-shaped line.

In order to detect lines of arbitrary widths, it is often necessary to iterate the detection procedure in the scale space. Conventionally, all lines in an image [1] are detected using a single optimal value of σ (big enough but not too big). Alternatively, the line is emphasized [8] by using the maximum response of all scales. Yet these methods are not entirely satisfactory. Figure 1 shows some examples of filter responses of different filter scales. The matched filter proposed in [1] is tested here. Figure 2 shows the filter responses to a bar-shaped line and a Gaussian-shaped line where f is the original signal and $M_\sigma f$ is the filter response at scale σ.

First, from Figure 2, we can see that there is a clear peak in both (a) and (b), which means only filters with particular scales can produce good responses to the lines with particular widths.

Second, as shown in Figure 1, because excessively wide filters will filter out small vessels and the vessels in retinal images can vary from very large to very small, it is rarely possible to find one single filter width value suitable for detecting all vessels.

Further, if the maximum response of all scales is selected, both the large and the small vessels can be emphasized but so too is the associated noise, as shown in Figure 1.

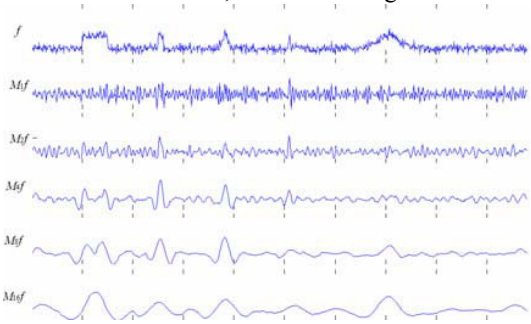

Figure 1 Filter responses of different scales

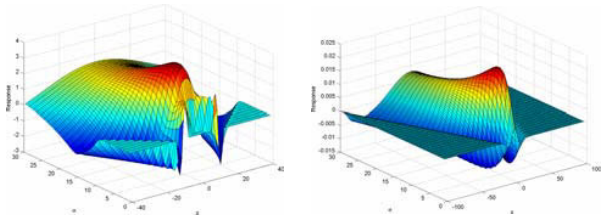

(a) **(b)**

Figure 2 Filter response along scale space (a) responses to bar-shaped line (b) responses to Gaussian-shaped line

From the analysis in last section, we can see that the traditional line detection methods cannot produce satisfactory results for vessel segmentation. We propose a multiscale analytical scheme for detecting all widths of vessels.

The idea of multiscale structure was first introduced by Mallat. In [13], he illustrated mathematically that signals and noise have different singularities and that edge structures present observable magnitudes along the scales, while noise decreases rapidly. Based on this observation, we applied this multiscale concept to solve problems of edge detection and noise by thresholding the multiscale products [14] [15].

Figure 3 shows the effects of scale multiplication. f is a signal corrupted by Gaussian white noise; $W_s f$ is the filter response at scale s; $P_s f$ is the product at two adjacent scales. Scale multiplication enhances the edges and filters noise.

In this paper, we further extend our multiscale approach to vessel detection. Our multiscale analytical scheme is summarized as follows.

1) Multiscale Gabor Filtering

We use a Gabor filter [16] here because it is capable of tuning in to specific frequencies and orientations. In most cases, only the real part of the Gabor filter is used for convolution with the modulation axis parallel to the envelope axis, which is expressed by

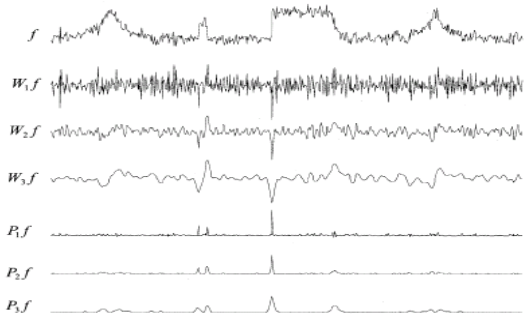

Figure 3. Multiscale edge detection and scale multiplication

$$g_\phi(x,y)=\exp\left\{-\pi\left(\frac{x'^2}{\sigma_x^2}+\frac{y'^2}{\sigma_y^2}\right)\right\}\cos\left(2\pi fx'\right) \quad (4)$$

$$x'=x\cos\phi+y\sin\phi \quad (5)$$

$$y'=-x\sin\phi+y\cos\phi \quad (6)$$

where ϕ is the filter direction, σ is standard deviation of Gaussian, and f is the frequency of cosine wave. (For convenience, the modulating Gaussians of filters are set to have the same direction as the complex sine grating so that there is only one direction parameter.)

For multiscale analysis, a scale parameter is added to equation (4) to control the filter size.

$$g_{\phi,s}(x,y)=\exp\left\{-\pi\left(\frac{x'^2}{(s\sigma_x)^2}+\frac{y'^2}{(s\sigma_y)^2}\right)\right\}\cos\left(2\pi fx'\right) \quad (7)$$

To produce a single peak response on the center of a line of width w using Gabor filters rotated in n directions, Liu [17] has proved that the parameters can be set as follows

$$f=\beta/w \quad (8)$$

$$\sigma_x=\frac{n\lambda w}{\alpha\beta\pi} \quad (9)$$

$$\sigma_y=\kappa\sigma_x \quad (10)$$

where $\alpha\in[1,1.5]$, $\beta\in[0.5,1]$, $\lambda=\sqrt{2\ln 2/\pi}$, and $\kappa=0.85$.

Adapting these to multiscale analysis, we modified equation (7) to

$$g_{\phi,s}(x,y)=\exp\left\{-\pi\left(\frac{x'^2}{s^2}+\frac{y'^2}{(\kappa s)^2}\right)\right\}\cos\left(2\pi fx'\right) \quad (11)$$

And

$$f=\frac{n\lambda}{\alpha\pi s} \quad (12)$$

Then, multiscale Gabor filtering can be applied in different directions with the optimal selection of s.

Figure 4 (a) shows a family of the Gabor filters defined above. The spatial frequency responses are illustrated in Figure 4 (b).

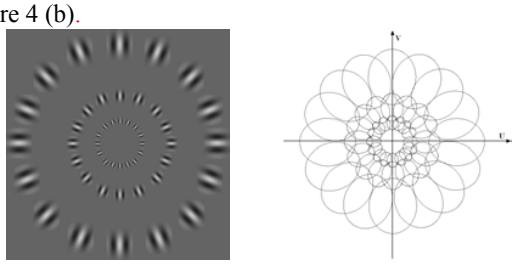

(a) **(b)**

Figure 4 A family of the Gabor filters with the spatial frequency responses

The response of Gabor filter can be expressed by

$$R_g(x,y)=g_{\phi,s}(x,y)*f(x,y) \quad (13)$$

where $f(x,y)$ is the image and $*$ is convolution.

2) Scale Selection

The scale multiplication is defined as the product of Gabor filter responses at two adjacent scales

$$P^{s_j}(x,y)=R_g^{s_j}(x,y)\cdot R_g^{s_{j+1}}(x,y) \quad (14).$$

The selection of parameter s is very important. In [15], the production of two adjacent scales produced good edge detection (illustrated in Figure 4). However, for line detection, the situation is different. Figure 6 shows some examples of scale multiplication for line detection where $P_{i,j}f$ is the production of scales i and j.

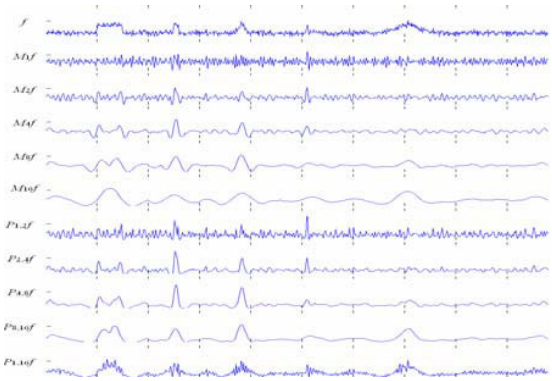

Figure 6. Multiscale line detection and scale multiplication

The following highlights some advantages of scale multiplication for line detection and the relevant illustration is shown in Figure 6.

- The filter responses to line are enhanced ($P_{2,4}f$, $P_{4,8}f$);
- The noises are reduced ($P_{2,4}f$, $P_{4,8}f$);
- The width of the line is enlarged by large scale filters, but this distortion can be corrected to the width at a smaller scale by multiply the responses at the large scale to the responses at a smaller scale ($P_{4,8}f$).

It should be pointed out that there are also some limitations of this approach as illustrated in Figure 6, which can be summarized as below:

- In the production of two small scale, there are nearly no responses to the large Gaussian-shaped line and vice versa ($P_{2,4}f$, $P_{8,16}f$)
- In the difference between two scales is very large, the responses of the production to both large and small Gaussian-shaped line are so weak that they are overwhelmed in the noises $P_{1,16}f$.

In order to make the scale multiplication applicable to line detection, the scale parameter should be carefully selected. The scales selected for multiplication must contain the information of lines with different widths.

In our case of retinal images, the widths of vessels vary from 3 to 16 pixels (most of the vessels). By plotting the filter peak responses to Gaussian-shaped lines with width 3 and 16, we find that there is a cross section, which can be used to guide the selection of scales. As shown in Figure 7, the most appropriate σ is around 0.8 to 2.2. The responses at other scales are too weak to work.

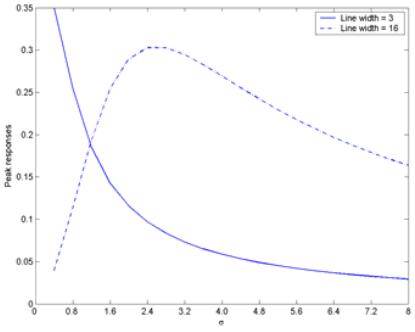

Figure 7. Filter peak responses along scale space

B. Extraction of Blobs, Optic Nerve, and Fovea

In this part, we use similar scheme with [20]. The Bright blobs are found in the image whose intensity is between 1.2 times the mean blood vessel intensity and 255, and dark blobs are extracted from images scaled between zero and 1.2 time's blood vessel intensity. The optic nerve is extracted as a fuzzy conversancy of blood vessels. The fovea is located 4.5mm temporal to the optic nerve a shown as a dark dot in the blue plane image.

III. CHANGE DETECTION

1) Fuzzy Post Classification Comparison (FPCC)

Our approach to Fuzzy Post Classification (FPCC) as a change detection method involves the independent fuzzy classification of digital images from different time intervala, then posing logical queries over those classified images. A fuzzy classifier has been implemented by an adaptation of the unsupervised fuzzy c-means clustering algorithm [25] in which the fuzzy class memberships are calculated using means and covariances determined from supervised training classes. This approach (using the reciprocal of the squared Mahalanobis distance) is favorably compared with posterior probability based approaches.

Our implementation is briefly described as follows:

- The Mahalanobis distance is computed of each pixel from the centroid for each class:

$$d^2_{ik} = (x_k - m_i)^T \sum_i^{-1} (x_k - m_i)$$

where d^2_{ik} represents the Mahalanobis distance between pixel x_k and the mean m_i of the *ith* class, superscript T denotes (vector) transpose and $\sum_i^{-1}$ is the inverse of the covariance matrix of the *ith* class.

- The fuzzy class membership of each pixel in the image in each class is computed:

$$\mu_{ik} = \frac{\left(1/d^2_{ik}\right)^m}{\sum_{j=1}^{c}\left(1/d^2_{ik}\right)^m}, \quad 1 \le k \le N$$

where μ_{ik} is the fuzzy class membership of pixel x_k in the class *i*, *c* is the number of classes, *N* is the total number of pixels in the image and *m* is a parameter used to control the degree of fuzziness of the class membership --- the theoretical properties of this parameter value are a key issue in the soft computing literature. Determining fuzzy class membership in this way ensures the unity sum condition $\sum_{i=1}^{c} \mu_{ik} = 1$ for all pixels *k*.

2) Hierarchical Change Detection

To reduce the computational complexity for change detection, we propose to perform feature pixel comparison in a hierarchical structure based on wavelet transform, starting from the coarse level (with few feature points) to a fine level (with more points). To avoid a blind pixel-wise comparison in the original images, our guided comparison algorithm applies Fuzzy Post Classification Comparison (FPCC) first at the low level, coarse grained feature images, to mark the possible regions of change. Those detected regions are then investigated at the higher level of the feature images for a final, and more accurate, output.

3) Categorization of Change

To identify the type of change as the indicative measure in medical diagnosis, we will combine fuzzy compactness and principal component analysis to reduce the redundant features for classification. Principal component analysis (PCA) is a technique that is often used to reduce redundancy and dimensionality of data. The principle of PCA is to find a set of m orthogonal vectors in the n-dimensional (n-D) data space that can account for as much as possible of the data's variance. Therefore, most of the intrinsic information in the data will be retained despite of a dimensionality reduction by projecting the data vectors from their original n-D space to the m-D space represented by the principal component vectors.

The most important information will be generated is the stage of diabite. Figure 8 shows the examples of diabetes in different stages.

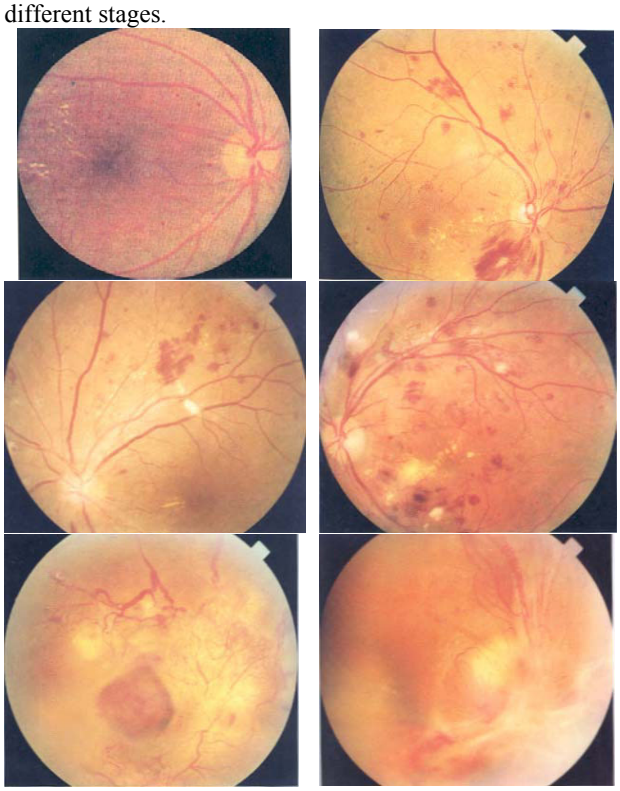

Figure 8 Diabetes from stage 1 to 6

IV. Experimental Results

Our experiments are conducted firstly on the STARE database [7] to compare to vessel detection performance.

The advantages of our approach for multiscale vessel segmentation over the performance of conventional methods as reported in STARE project [7] are demonstrated in Figure 9. The first row is the original retinal images in STARE database; the second row is the hand-labeled images as ground truth; the third row is the segmentation results by [7]; the last row is the segmentation results of our method. We can see that a number of small vessels missed by STARE are detected by our method. Note also that some vessels recorded as broken by [7] are connected when our method is used.

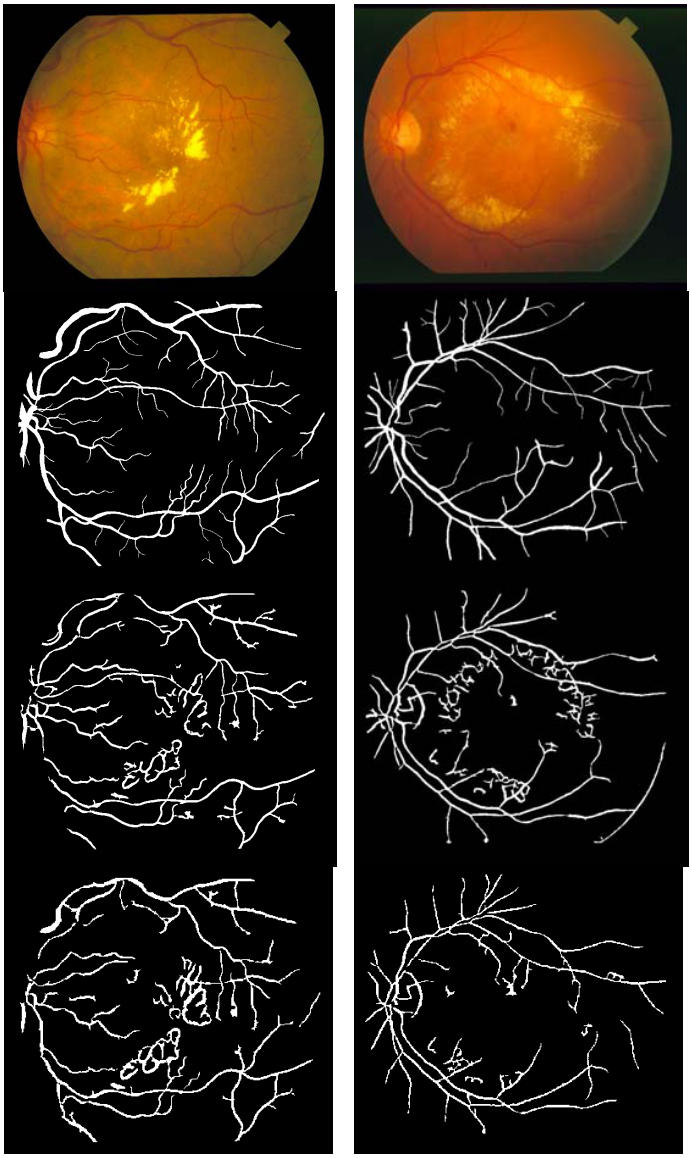

Figure 9 Vessel detection

The performance comparison is further illustrated by ROC curve in Figure 10. Our technique achieves better performance in both normal and abnormal retinal images.

Figure 11 gives some examples of Neovascularization detected by our system, which is an important sign for Proliferative Diabetic Retinopathy.

To test the change detection performance of our system, we established a retinal image database. Our database has 7 patients, each of them has 3~12 sets images which are taken at different times and each set has 4 images. We use the same setting as [7], the images were digitized at 700x605 pixels, 8 bits per color channel. Based on this database, we achieve

the diabetic stage reorganization rate at 73.6 %

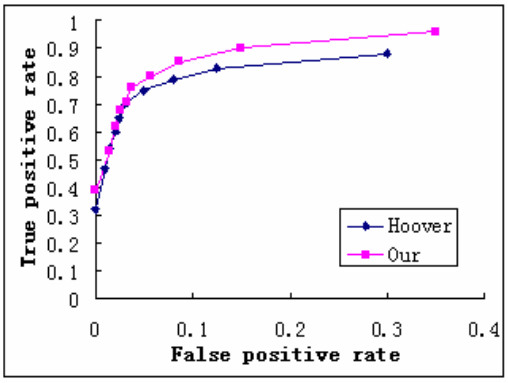

Figure10 Performance evaluation using ROC curve

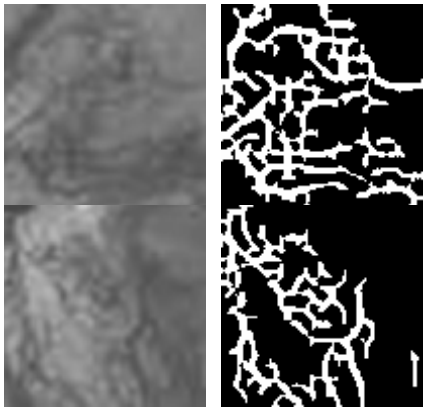

Figure11 Neovascularization detected

V. CONCLUSION

We conclude that our system for object extraction and change detection in retinal images is effective to help eye specialists to evaluate treatments and implement better clinical studies. Due to the limited resources, we can not achieve high diabetic stage recognition rate. However, due to the high quality of extraction of some objects in retinal images, the change detection can still provide useful information

REFERENCES

[1] S. Chaudhuri, S. Chatterjee, N. Katz, M. Nelson, and M. Goldbaum, "Detection of blood vessels in retinal images using two-dimensional matched filters," *IEEE Trans. Med. Imag.*, vol. 8, pp. 263–269, Sept. 1989.

[2] T. Pappas and J. Lim, "A new method for estimation of coronary artery dimensions in angiograms," *IEEE Trans. Acoust., Speech, Signal Processing*, vol. 36, pp. 1501–1513, Sept. 1988.

[3] Pinz, S. Bernogger, P. Datlinger, and A. Kruger, "Mapping the human retina," *IEEE Trans. Med. Imag.*, vol. 17, pp. 606–619, Aug. 1998.

[4] Y. Sun, "Automated identification of vessel contours in coronary arteriograms by an adaptive tracking algorithm," *IEEE Trans. Med. Imag.*, vol. 8, pp. 78–88, Mar. 1989.

[5] S. Tamura, Y. Okamoto, and K. Yanashima, "Zero-crossing interval correction in tracing eye-fundus blood vessels," *Pattern Recognit.*, vol. 21, no. 3, pp. 227–233, 1988.

[6] Y. Tolias and S. Panas, "A fuzzy vessel tracking algorithm for retinal images based on fuzzy clustering," *IEEE Trans. Med. Imag.*, vol. 17, pp. 263–273, Apr. 1998.

[7] A. Hoover, V. Kouznetsova, and M. Goldbaum, "Locating blood vessels in retinal images by piecewise threshold probing of a matched filter response," *IEEE Trans. on Medical Imaging*, vol. 19, no. 3, pp. 203–210, 2000.

[8] T.M. Koller, G. Gerig, G. Székely, and D. Dettwiler, "Multiscale Detection of Curvilinear Structures in 2-D and 3-D Image Data," *Fifth Int'l Conf. Computer Vision,* pp. 864-869. Los Alamitos, Calif: IEEE CS Press, 1995.

[9] J.B. Subirana-Vilanova and K.K. Sung, "Multi-Scale Vector-Ridge-Detection for Perceptual Organization Without Edges," A.I. Memo 1318, MIT Artificial Intelligence Lab., Cambridge, Mass., Dec. 1992.

[10] J.B.A. Maintz, P.A. van den Elsen, and M.A. Viergever, "Evaluation of Ridge Seeking Operators for Multimodality Medical Image Matching," *IEEE Trans. Pattern Analysis and Machine Intelligence*, vol. 18, no. 4, pp. 353-365, Apr. 1996.

[11] L. Wang and T. Pavlidis, "Direct Gray-Scale Extraction of Features for Character Recognition," *IEEE Trans. Pattern Analysis and Machine Intelligence*, vol. 15, no. 10, pp. 1,053-1,067, Oct. 1993.

[12] L.A. Iverson and S.W. Zucker, "Logical/Linear Operators for Image Curves," *IEEE Trans. Pattern Analysis and Machine Intelligence*, vol. 17, no. 10, pp. 982-996, Oct. 1995.

[13] S. Mallat and S. Zhong, "Characterization of signals from multiscale edges," *IEEE Trans. Pattern Anal. Machine Intell.*, vol. 14, pp. 710–732, July 1992.

[14] P. Bao and L. Zhang, "Noise Reduction for Magnetic Resonance Image via Adaptive Multiscale Products Thresholding," *IEEE Trans. Medical Imaging,* vol. 22, pp. 1089-1099, Sept. 2003.

[15] P. Bao, L. Zhang, and X. L. Wu, "Canny Edge Detection Enhancement by Scale Multiplication", *IEEE Trans. Pattern Analysis and Machine Intelligence*, Vol. 27, No. 9, Sept. 2005

[16] J.G. Daugman, "Uncertainty relation for resolution in space, spatial frequency, and orientation optimized by two-dimensional visual cortical filters," *Journal of the Optical Society of America A*, vol. 2, pp. 1160-1169, 1985.

[17] Z.-Q. Liu, J. Cai, and R. Buse, *Handwriting Recognition: Soft Computing and Probabilistic Approaches*, pp. 31-57, Springer, Berlin, 2003

[18] S. Chaudhuri, S. Chatterjee, N. Katz, M. Nelson, M. Goldbaum, "Detection of Blood Vessels in Retinal Images Using Two-Dimensional Matched Filters," *IEEE Transactions on Medical Imaging*, vol. 8, pp. 263-269, 1989.

[19] M.H. Goldbaum, B.L CetC, R.F. Garcia, W.E. Hart, P. Kube, M. Nelson, "Computer Detection and Classification of Lesions Found in Diabetic Retinopathy," *Invest Ophthalmol Vis Sci*, vol. 33, p. 1082, 1992.

[20] Goldbaum, M., Moezzi, S., Taylor, A., Chatterjee, S., Boyd, J., Hunter, E., and Jain, R. 'Automated diagnosis and image understanding with object extraction, object classification, and inferencing in retinal images'. *In IEEE Int. Conf. on Image Processing*. Vol. 3. pp. 695-698, 1996

[21] P. Deer, ``Digital change detection techniques: Civilian and military applications," Proc. of International Symposium for Spectral Sensing Research, 1995.

[22] R. Weismiller, S. Kristof, D. Scholz, P. Anuta and S. Momin, ``Change detection in coastal zone environments," Photogrammetric Engineering and Remote Sensing, vol. 43, pp. 1533-1539, 1977.

[23] A. Singh, ``Digital change detection techniques using remotely-sensed data," International Journal of Remote Sensing, vol. 10, pp. pp. 989-1003, 1989.

[24] P. Pilon, P. Howarth, R. Bullock and P. Adeniyi, ``An enhanced classification approach to change detection in the semi-arid environments," Photogrammetric Engineering and Remote Sensing, vol. 55, pp. 1709-1716, 1988.

[25] J. Bezdek, R. Ehrlich and W. Full, ``FCM: The fuzzy c-means clustering algorithm," *Computers and Geoscience*, vol. 10, pp. 191-203, 1984.